



## BASIC SCIENCE ARTICLE

# $\alpha$ 1,3-Fucosyltransferase-IX, an enzyme of pulmonary endogenous lung stem cell marker SSEA-1, alleviates experimental bronchopulmonary dysplasia

Sushma Chaubey<sup>1,4</sup>, Yaldah Mohammad Nader<sup>1</sup>, Dilip Shah<sup>1,5</sup>, Ogan K. Kumova<sup>2</sup>, Varsha Prahaladan<sup>1</sup>, Alison J. Carey<sup>1,2</sup>, Sture Andersson<sup>3</sup> and Vineet Bhandari<sup>1,5</sup>

**BACKGROUND:** Endogenous pulmonary stem cells (PSCs) play an important role in lung development and repair; however, little is known about their role in bronchopulmonary dysplasia (BPD). We hypothesize that an endogenous PSC marker stage-specific embryonic antigen-1 (SSEA-1) and its enzyme,  $\alpha$ 1,3-fucosyltransferase IX (FUT9) play an important role in decreasing inflammation and restoring lung structure in experimental BPD.

**METHODS:** We studied the expression of SSEA-1, and its enzyme FUT9, in wild-type (WT) C57BL/6 mice, in room air and hyperoxia. Effects of intraperitoneal administration of recombinant human FUT9 (rhFUT9) on lung airway and parenchymal inflammation, alveolarization, and apoptosis were evaluated.

**RESULTS:** On hyperoxia exposure, SSEA-1 significantly decreased at postnatal day 14 in hyperoxia-exposed BPD mice, accompanied by a decrease in FUT9. BPD and respiratory distress syndrome (RDS) in human lungs showed decreased expression of SSEA-1 as compared to their term controls. Importantly, intraperitoneal administration of FUT9 in the neonatal BPD mouse model resulted in significant decrease in pulmonary airway (but not lung parenchymal) inflammation, alveolar–capillary leakage, alveolar simplification, and cell death in the hyperoxia-exposed BPD mice.

**CONCLUSIONS:** An important role of endogenous PSC marker SSEA-1 and its enzyme FUT9 is demonstrated, indicating early systemic intervention with FUT9 as a potential therapeutic option for BPD.

*Pediatric Research* (2021) 89:1126–1135; <https://doi.org/10.1038/s41390-020-0891-9>

**IMPACT:**

- Administration of rhFUT9, an enzyme of endogenous stem cell marker SSEA-1, reduces pulmonary airway (but not lung parenchymal) inflammation, alveolar–capillary leak and cell death in the BPD mouse model.
- SSEA-1 is reported for the first time in experimental BPD models, and in human RDS and BPD.
- rhFUT9 treatment ameliorates hyperoxia-induced lung injury in a developmentally appropriate BPD mouse model.
- Our results have translational potential as a therapeutic modality for BPD in the developing lung.

**INTRODUCTION**

Bronchopulmonary dysplasia (BPD) is a chronic lung disease in premature infants treated with supplemental oxygen after birth.<sup>1</sup> It is more common in infants with low birth weight who receive prolonged mechanical ventilation to treat respiratory distress syndrome (RDS), caused by insufficient surfactant production and immaturity of the lung. The hallmark of BPD is alveolar simplification and dysregulated vascularization.<sup>2</sup> Although significant progress has been made to improve the morbidity and mortality of this disease, it remains a serious condition, which is extremely challenging to manage.<sup>3</sup> There is no single effective treatment for BPD.

The possibility that endogenous stem/progenitor cells could modulate the immune system has led to an increasing interest in

using stem/progenitor cells as a potential therapeutic modality for BPD.<sup>4,5</sup> Endogenous stem and progenitor cell populations are well described in many tissues, including lung, which contains discrete progenitor populations that respond to various types of injury.<sup>6</sup> Mesenchymal stem cell (MSC) therapy in a model of lung injury has been reported to result in an increase in the number of bronchoalveolar SC (BASC) providing a plausible mechanism of the repair of the injured alveolus.<sup>7</sup> Previous studies have indicated that primary neonatal pulmonary epithelial cells express stage-specific embryonic antigen-1 (SSEA-1).<sup>8</sup> SSEA-1, also known as Lewis X or CD15, is a well-known carbohydrate antigenic epitope, selectively expressed on mouse embryonic cells, and on certain fetal and adult tissues. It is expressed on undifferentiated cells and

<sup>1</sup>Section of Neonatal-Perinatal Medicine, Department of Pediatrics, Drexel University College of Medicine, Philadelphia, PA, USA; <sup>2</sup>Department of Microbiology and Immunology, Drexel University College of Medicine, Philadelphia, PA, USA and <sup>3</sup>Department of Neonatology, University of Helsinki and Helsinki University Hospital, Children's Hospital, Helsinki, Finland  
Correspondence: Vineet Bhandari (bhandari-vineet@cooperhealth.edu)

<sup>4</sup>Present address: Department of Biomedical Engineering, Widener University, One University Place, Chester, PA, USA

<sup>5</sup>Present address: Neonatology Research Laboratory (Room #206), Cooper University Hospital, Education and Research Building, Camden, NJ, USA

Received: 16 May 2019 Revised: 19 February 2020 Accepted: 19 March 2020

Published online: 17 April 2020

has been recognized as a neural stem cell and endogenous PSC marker.<sup>8–10</sup> SSEA-1 moiety is involved in cell–cell interactions, cell migration, adhesion, and process formation.<sup>11</sup> SSEA-1 is synthesized by transferring a fucose residue from GDP-fucose to *N*-acetylglucosamine by the action of  $\alpha$ 1,3-fucosyltransferase-IX (FUT9).<sup>12</sup> The aim of this study was to detect the expression of SSEA-1<sup>+</sup> PSC in the lungs of neonatal mice and humans and to investigate the therapeutic potential of an enzyme of SSEA-1, FUT9, in the progression of experimental BPD.

## MATERIALS AND METHODS

### Animals

Wild-type (WT) C57BL/6 mice were obtained from The Jackson Laboratory (Bar Harbor, Maine, USA) and were maintained in a breeding colony at Drexel University, Philadelphia. Animal procedures were performed in accordance to the NIH Guide for the care and use of laboratory animals and were approved by the Institutional Animal Care and Use Committee of Drexel University.

### Oxygen exposure and mouse model of BPD

Newborn (NB) pups were exposed to hyperoxia, along with their mothers, in cages in an airtight Plexiglas chamber (OxyCycler; Biospherix, Redfield, NY) as described previously by our group.<sup>13,14</sup> Exposure to >95% oxygen from birth until postnatal day 4 (PN4) corresponds to the sacular stage of mouse lung development. On PN5, all animals were placed in room air (RA) up to PN14, which corresponds to the alveolar stage of mouse lung development, to allow for a period of recovery. Using this experimental model, NB WT mouse lungs at PN14 have the phenotype mimicking severe BPD in humans.

We utilized another model that mimics the BPD pulmonary phenotype as an additional model of lung injury (NB WT doxycycline-inducible vascular endothelial growth factor (VEGF) transgenic (TG) mice under RA conditions at PN7,<sup>15</sup> as evidenced by increased chord length and vascular permeability).

### Injection of rhFUT9 into the neonatal mouse BPD model

Recombinant human FUT9 (rhFUT9) protein of 2.5  $\mu$ g, resuspended in total 100  $\mu$ l of phosphate-buffered saline (PBS), was injected via the intraperitoneal (i.p.) route into each neonatal mouse at PN2 and PN4 in our BPD model. The same volume of phosphate-buffered saline (PBS) served as control injections. There is no known therapeutic FUT9 dose at present. To the best of our knowledge, this is the first study that demonstrates the effect of FUT9 in BPD mice. Our rationale for choosing this dose was based on previous studies in mice by us<sup>14</sup> and others.<sup>16</sup>

Bronchoalveolar lavage (BAL), tissue processing, Western blot analysis, terminal deoxynucleotidyl transferase dUTP nick end labeling (TUNEL) assay, immunofluorescence and immunohistochemistry, isolation of pulmonary parenchymal immune cells, flow cytometry, and heart measurements for pulmonary hypertension (PH)-induced right ventricular hypertrophy (RVH) have been described in Supplementary Information: Experimental Procedures (online).

### Lung morphometry

Mice were killed by an i.p. injection with an overdose of xylazine/ketamine. The trachea was cannulated, and the lungs were fixed with 4% paraformaldehyde at 25 cm H<sub>2</sub>O inflation pressure for 15 min. Lungs were dissected and whole lungs were fixed overnight in 4% paraformaldehyde and subsequently embedded in paraffin. Five-micrometer-thick paraffin-embedded sections were stained with hematoxylin and eosin. A minimum of five randomly chosen areas from each section were photographed with the  $\times$ 200 magnification. Investigators were blinded to experimental groups for the analysis. Alveolar size was estimated from the mean chord length of the airspace, as described

previously.<sup>13</sup> The mean alveolar area was calculated using the method previously reported.<sup>17</sup> The number of branches, junctions, triple points, quadruple points, junction voxels, and end points voxels were calculated using AnalyzeSkeleton program from ImageJ. This plugin tags all pixel/voxels in a skeleton image and then counts all its junctions, triple and quadruple points, and branches. Junction voxels are defined by having more than two neighbors. The number of triple points and quadruple points depicts those cells having more than three or four neighbors, respectively.

### Collection and processing of human lung tissues from term, RDS, and BPD babies

Human lung samples were obtained post mortem, from premature infants having the diagnosis of RDS 1–2 days, RDS 3–7 days, RDS > 7 days, BPD and term controls. Informed consent was obtained, and the collection and processing of the human lung samples was approved by the National Supervisory Authority for Welfare and Health in Finland and the University of Rochester Institutional Review Board. Selected clinical details have been shown in Supplementary Table S1 (online).

### Statistical analysis

All statistical analyses were performed using the Prism 7.0 software (GraphPad for windows, San Diego, CA). Dual comparisons were made using unpaired two-tailed *t* test and *p* < 0.05 was regarded as significant. Groups of three or more were analyzed by one-way analysis of variance, followed by Tukey's post hoc test for experiments comparing treatments to controls. Statistical significance was defined as *p* < 0.05. Mean values were expressed as mean  $\pm$  SEM. The number of mice per group is indicated in the legend of each figure.

## RESULTS

### Hyperoxia decreases SSEA-1 expression in the lungs of BPD mice at PN14

Western blot was done to determine the expression level of SSEA-1 in the lungs of RA and BPD mice at PN14. SSEA-1 expression was significantly decreased in BPD lung samples compared to the RA samples at PN14 (Fig. 1a). Immunohistochemistry also showed significant decrease in SSEA-1<sup>+</sup> cells in BPD compared to RA lungs (Supplementary Fig. S1A–D online). SSEA-1<sup>+</sup> cells colocalizes with surfactant protein-C (SP-C), a highly specific marker for identifying type II alveolar epithelial cells in lungs. SP-C is a known cell surface stem cell marker expressed on neonatal SSEA-1<sup>+</sup> PSC.<sup>8</sup> We show a significant decrease in the SSEA-1/SP-C double-positive cells in BPD compared to RA lungs (Supplementary Fig. S1A, B, D online).

SSEA-1 expression was studied in the additional experimental model that mimics the BPD pulmonary phenotype (NB WT doxycycline-inducible VEGF TG mice under RA conditions at PN7). The VEGF TG mice show a BPD-like phenotype, including increased chord length and vascular permeability.<sup>15</sup> SSEA-1 was decreased in WT VEGF TG RA PN7 mice lungs (Supplementary Fig. S2 online), which correlates to the results obtained in BPD mice (Fig. 1a). The result also indicates that SSEA-1 may be modulated by VEGF. The role of VEGF in modulating this response needs further studies.

### Human RDS and BPD lung tissues demonstrate decreased expression of SSEA-1 as compared to their term control counterparts

To evaluate SSEA-1 expression in RDS and BPD human lungs, we stained human lung sections for SSEA-1. We demonstrated significantly decreased levels of SSEA-1 in the RDS and BPD groups compared to term control groups (Fig. 1b, c). This clinical result corresponds to our BPD mouse lung data, suggesting that the decrease in SSEA-1 expression in BPD mice may be associated with inflammation in hyperoxia-induced lung injury.

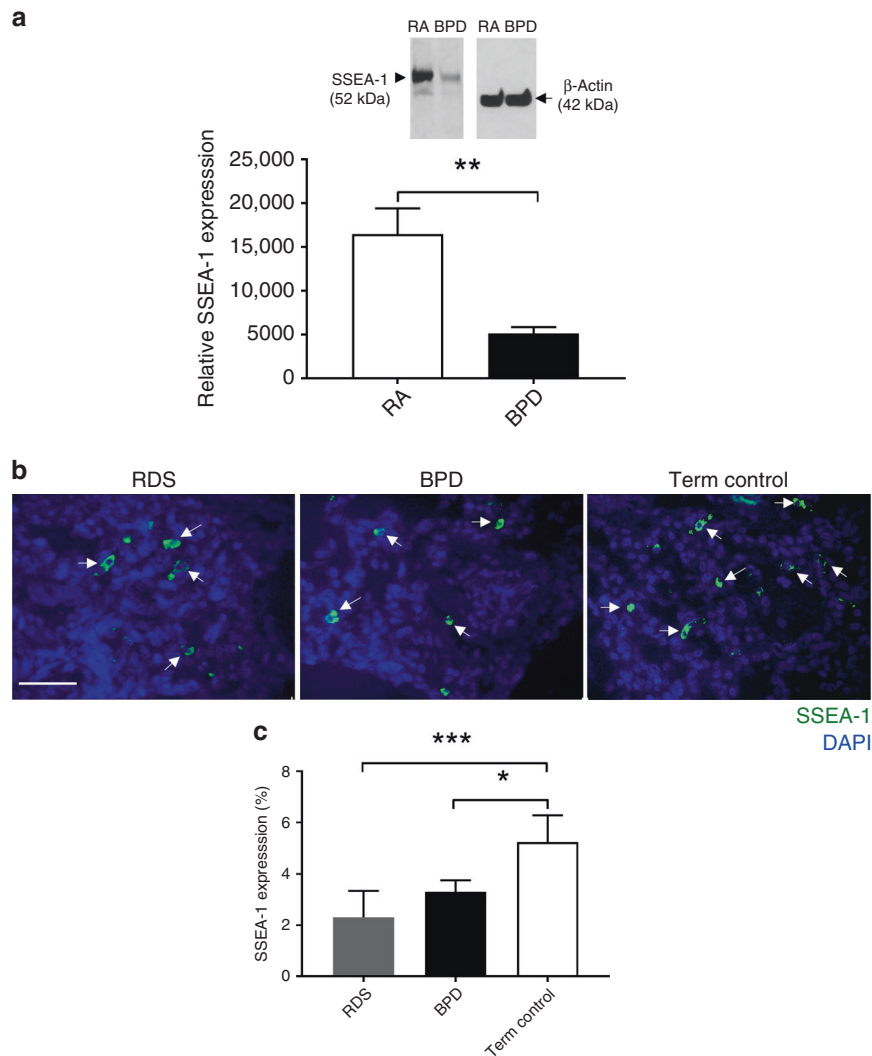


**Fig. 1 Expression of SSEA-1 in the lungs of RA and BPD mice at PN14, and human RDS and BPD lungs and their term control counterparts.** **a** Hyperoxia decreases the expression of SSEA-1 in the lungs of BPD mice at PN14. Western blotting and quantitation of SSEA-1 expression in RA and BPD groups at PN14. Significant decrease in the expression of SSEA-1 (~55 kDa) was detected in the BPD lung lysates compared to RA lung lysates at PN14.  $\beta$ -Actin (42 kDa) was used as loading controls for quantitation of SSEA-1 expression by densitometry. **b** Representative SSEA-1 immunofluorescence images of RDS (I), BPD (II), and term control (III) human lung. SSEA-1-positive cells are labeled with fluorescein isothiocyanate (FITC) (green). The nuclei are counterstained with DAPI. Arrows depict SSEA-1-positive cells in the field. Scale bar: 50  $\mu$ m. **c** Histogram depicting the quantitative analysis of SSEA-1-positive cells in the human lungs of RDS, BPD, and term controls. All values are expressed as mean  $\pm$  SEM;  $N=3-5$  mice per group or 3-5 human samples per group; one-way ANOVA with Tukey's post hoc correction; \* $p < 0.05$ ; \*\* $p < 0.01$ ; \*\*\* $p < 0.001$ .

#### Expression of Pax 6, FUT9, Msi-1, Numb, and Notch-1 in RA vs. BPD samples

Cell surface glycoconjugates, including glycoproteins, glycolipids, and proteoglycans, play important functional roles in stem cell maintenance.<sup>10</sup> Studies on neural stem cells show downregulation of FUT9 in cells that are differentiated from neural SC.<sup>18</sup> SSEA-1, which account for 20% of the total N-glycans in NSC, also disappears during differentiation.<sup>19</sup> Msi-1 plays a crucial role in maintaining the undifferentiated state of stem cells via activation of the Notch signaling pathway.<sup>20,21</sup> Pax 6 controls the expression of FUT9 and is known to promote proliferation of neural progenitor cells and neurogenesis.<sup>22</sup> A postulated pathway depicting how hyperoxia acts as an active modulator of glycoconjugates and Notch signaling, resulting in decreased cell proliferation and increased cell death, is shown in Fig. 2a. We performed Western blotting to detect expression levels of different upstream and downstream proteins of SSEA-1 at PN14 in RA and BPD mouse lung samples. We found that hyperoxia

downregulated the expression of upstream proteins, Pax 6 (Fig. 2b) and FUT9 (Fig. 2c). We have shown earlier that there is downregulation of SSEA-1 in BPD (Fig. 1). Next, we noted a decrease in downstream protein, Msi-1 (Fig. 2d), and an increase in Numb protein (Fig. 2e). Numb protein is known to bind Notch-1 protein and inhibit the activation of the Notch signaling pathway, resulting in decreased expression of Notch-1 (Fig. 2f).

FUT9 treatment reverses hyperoxia-induced pulmonary inflammation and alveolar-capillary leak in the BPD mouse. We found that hyperoxia exposure decreased the expression of FUT9, a key enzyme for the synthesis of SSEA-1, an endogenous PSC marker. We hypothesized that injection of FUT9 would affect endogenous stem cell proliferation and might have therapeutic potential. To determine if hyperoxia-induced lung inflammation responds to FUT9, we performed i.p. injections of rhFUT9 into pups (at PN2 and PN4) exposed to hyperoxia (>95% O<sub>2</sub>). After 4 days hyperoxia exposure from birth to PN4, these pups were

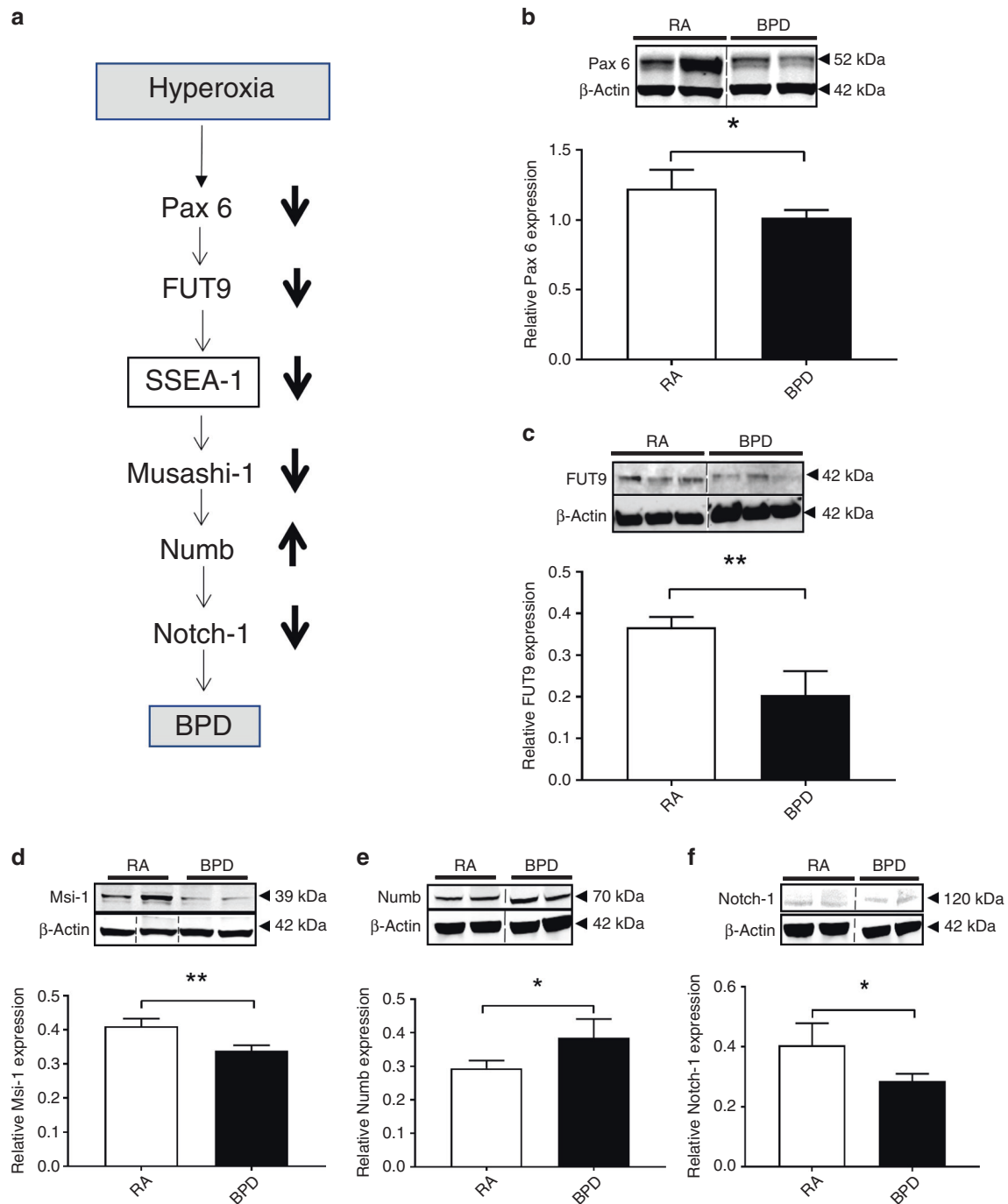


**Fig. 2** Hyperoxia decreases the expression of Pax 6, FUT9, Msi-1, and Notch-1 and increases the expression of Numb in BPD lungs as compared to RA lungs at PN14. **a** Schematic representation of proposed SSEA-1 pathway in BPD pathology. On hyperoxia exposure, FUT9, an enzyme of SSEA-1, decreases the expression of SSEA-1 and operates as a deactivator of Notch signaling pathway, resulting in decreased proliferation and increased cell death during lung development. **b–f** Western blotting and quantitation of Pax 6, FUT9, Msi-1, Numb, and Notch-1 in RA and BPD groups at PN14.  $\beta$ -Actin was used as loading controls for quantitation of expression of all proteins by densitometry. **b–d** Western blotting and quantitation of Pax 6, FUT9, and Msi-1 in RA and BPD groups at PN14. Significant decrease in the expression of Pax 6 (~52 kDa), FUT9 (42 kDa), and Msi-1 (~39 kDa) was detected in the BPD lung lysates compared to RA lung lysates. **e** Western blotting and quantitation of Numb expression in RA and BPD groups at PN14. Significant increase in the expression of Numb (~75 kDa) was detected in the BPD lung lysates compared to RA lung lysates. **f** Western blotting and quantitation of Notch-1 expression in RA and BPD groups at PN14. Significant decrease in the expression of Notch-1 (~120 kDa) was detected in the BPD lung lysates compared to RA lung lysates. All values are expressed as mean  $\pm$  SEM;  $N = 3$ –4 mice per group; one-way ANOVA with Tukey's post hoc correction; \* $p < 0.05$ ; \*\* $p < 0.01$ .

placed at RA till PN14 as defined in our hyperoxia-induced BPD mouse model<sup>13,14</sup> (Fig. 3a). The control group comprises pups exposed to the same hyperoxia conditions and injected with vehicle (PBS) at PN2 and PN4. FUT9 injections in BPD mice resulted

in significantly higher body weight compared to RA-, BPD-, or PBS-injected groups (Fig. 3b). On hyperoxia exposure, total cell count in BAL fluid (BALF) in BPD mice was significantly increased compared to that in RA, demonstrating accumulation of

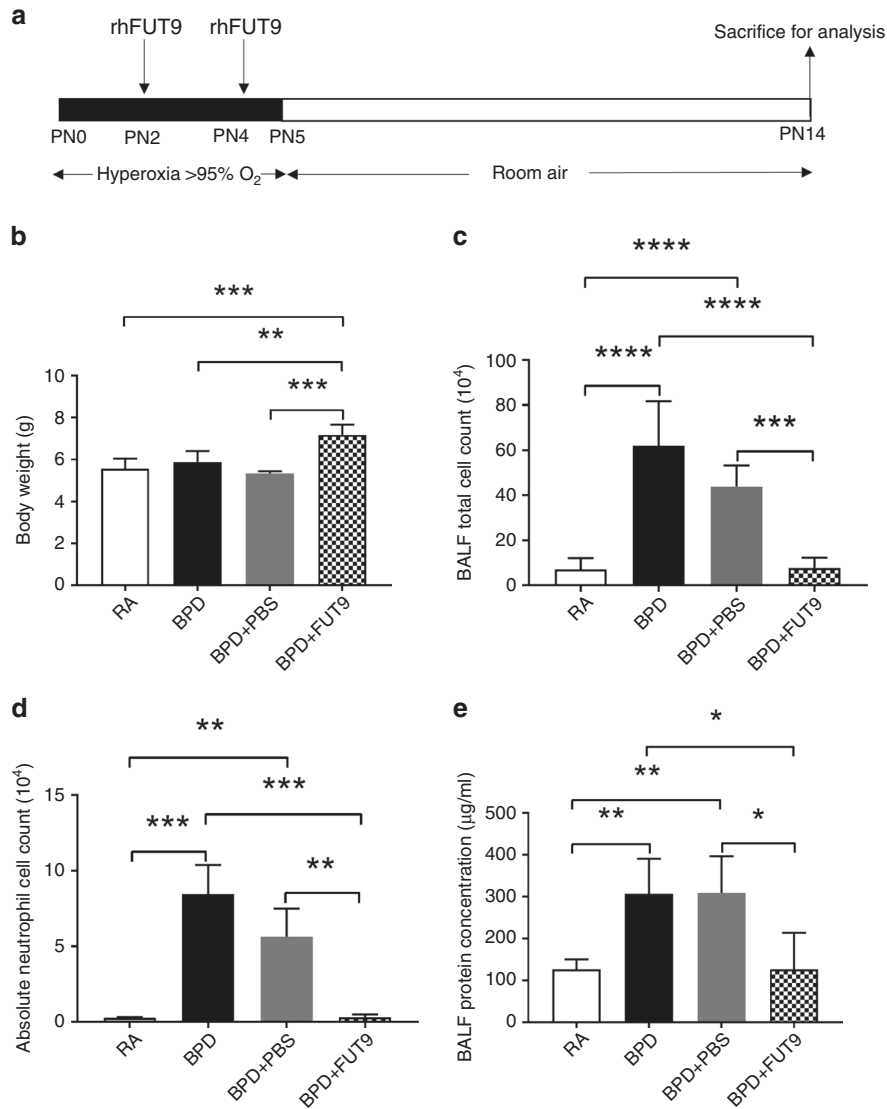


**Fig. 3** FUT9 treatment reverses pulmonary inflammation and alveolar–capillary leak associated with hyperoxia-induced lung injury in the BPD mouse model. **a** Schematic representation of BPD mouse model and FUT9 injection regime. The mice were kept in 100% oxygen from birth to PN4, followed by RA exposure till PN14. The mice were sacrificed for analysis at PN14. Intraperitoneal injections of FUT9 were given at PN2 and PN4. **b–d** Histogram showing animal body weight (**b**), BALF total cell count (**c**), BALF absolute neutrophil count (**d**), BALF protein concentration (**e**), in RA, BPD, and vehicle (PBS)- and FUT9-injected BPD mice at PN14. All values are expressed as mean ± standard error of the mean (SEM); four experiments, *N* = 3–6 mice per group; one-way ANOVA with Tukey’s post hoc correction; \**p* < 0.05; \*\**p* < 0.01; \*\*\**p* < 0.001; \*\*\*\**p* < 0.0001.

inflammatory cells upon injury (Fig. 3c). However, with FUT9 treatment, BALF total cell counts were statistically decreased to RA levels (Fig. 3c). No significant decrease in BALF total cell counts was observed in BPD mice injected with the vehicle (PBS). Similarly, there was a significant increase in infiltration of neutrophils, as assessed by the absolute neutrophil counts, in BALF of BPD compared to RA. This increase in neutrophil counts in BPD mice was blocked on treatment with FUT9 (Fig. 3d).

Hyperoxia-induced lung injury is characterized by endothelial cell damage and disruption of the alveolar–capillary barrier, leading to increased protein leak in the BALF. To determine the extent of capillary leakage, the protein concentration in BALF was measured (Fig. 3e). There was a statistically significant increase in BALF protein in BPD vs. RA. This increase in total BALF protein in BPD was not diminished on treatment with PBS; however, FUT9 treatment significantly decreased the protein leak. In summary, our results show that FUT9 treatment significantly suppressed inflammatory cell accumulation specifically in the BASC and has a

protective role in the maintenance of the alveolar–capillary barrier in the presence of hyperoxia.

FUT9 treatment reverses alveolar injury and other morphometric alterations associated with hyperoxia-induced lung injury in the BPD mouse

Impaired alveolar growth, as evidenced by fewer and larger alveoli with heterogeneous sizes, was observed in BPD compared to RA lungs. These impairments in alveolar growth and morphological changes observed in BPD were attenuated in the FUT9-injected pups but not in PBS-injected pups (Fig. 4a). Based on morphometric analysis, the chord length, which is indicative of alveolar size, was significantly higher in BPD as compared to RA groups. This hyperoxia-induced increase in mean chord length was significantly ameliorated by FUT9 treatment (Fig. 4b).

Alveolar area was significantly increased in BPD compared to RA lungs. Injecting the BPD mice with the vehicle (PBS) had no effect. However, alveolar area was significantly reduced to the RA levels

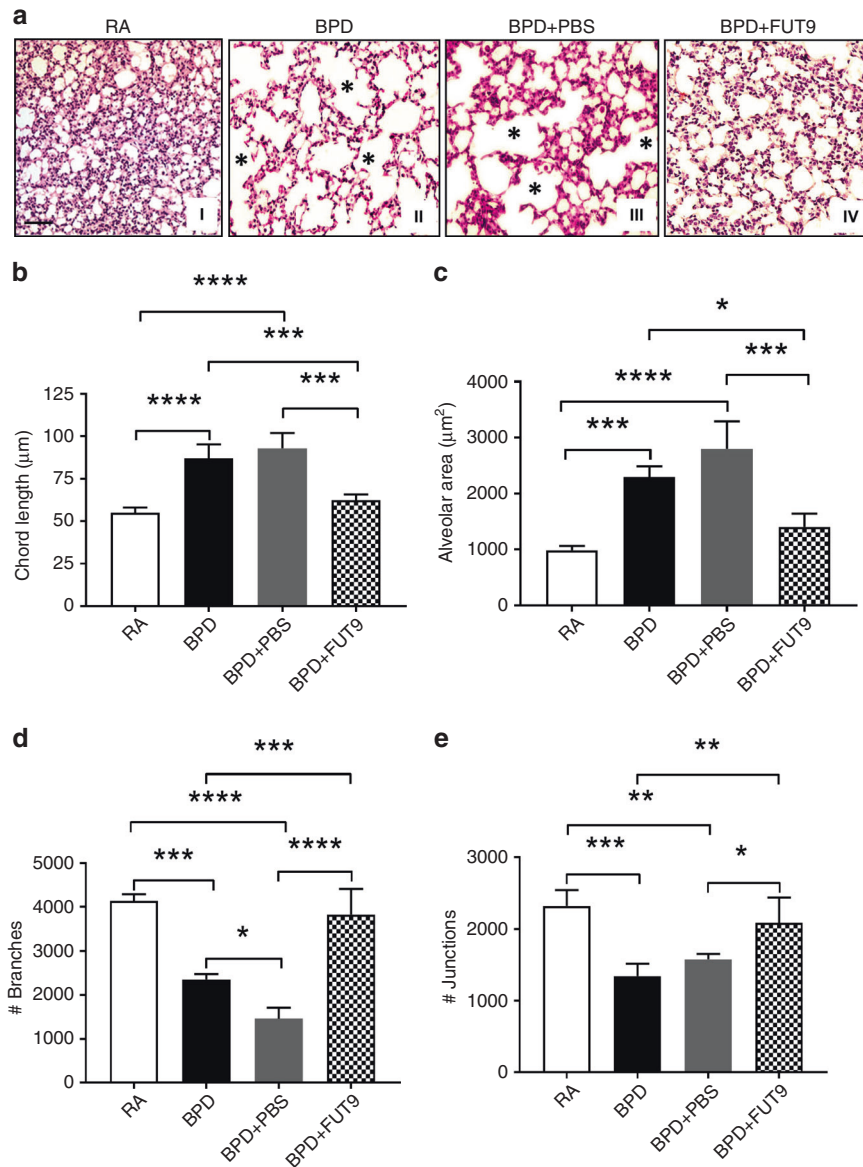


**Fig. 4** FUT9 treatment reverses altered lung morphology associated with hyperoxia-induced lung injury in the BPD mouse model. **a** Representative images of lung histology with H&E stain from the four experimental groups, RA (I), BPD (II), BPD + PBS (III), and BPD + FUT9 (IV). Asterisks depict the increased alveolar simplification in the BPD- and PBS-injected mice as compared to RA. Magnification  $\times 200$ , scale bar: 50  $\mu\text{m}$ . **b–e** Histogram depicting the mean chord length (**b**), alveolar area (**c**), number of branches (**d**), number of junctions (**e**) in lungs of RA, BPD, and PBS-, or FUT9-injected BPD mice at PN14. All values are expressed as mean  $\pm$  standard error of the mean (SEM); four experiments,  $N = 3\text{--}4$  mice per group; one-way ANOVA with Tukey's post hoc correction; \* $p < 0.05$ ; \*\* $p < 0.01$ ; \*\*\* $p < 0.001$ ; \*\*\*\* $p < 0.0001$ .

after FUT9 injections in BPD mice (Fig. 4c). Further in-depth analysis of other lung morphological parameters, such as number of branches, junctions (Fig. 4d, e), triple and quadruple points, and junction and end point voxels (Supplementary Fig. S3 online), was performed. Interestingly, we found that FUT9 treatment attenuated the morphological alterations in BPD mouse (Fig. 4, Supplementary Fig. S3 online). There was no change in alveolar area in the RA mice injected with FUT9, when compared to RA alone (Supplementary Fig. S4A, B online). To summarize, FUT9 treatment significantly improved pulmonary architecture in the hyperoxia-induced mouse BPD model.

FUT9 treatment decreases cell death and increases the expression of SSEA-1 in BPD lungs  
To further assess the mechanism of the improved architecture in lung tissue, we evaluated apoptosis using TUNEL staining.

Hyperoxia causes oxidant-induced DNA injury and cell death, which results in increased pulmonary tissue TUNEL staining. The percentage of TUNEL-positive dead cells was seen significantly increased in the BPD mice compared to RA (Fig. 5a, b). FUT9 treatment significantly decreased hyperoxia-induced cell death in the lungs of the BPD mice (Fig. 5a, b). In addition, there was a significant increase in expression of the cell proliferation marker, Ki67, in the FUT9-injected BPD mice as compared to BPD or the vehicle/PBS-injected mice at PN14 (Supplementary Fig. S4C, D online).

FUT9 is essential for the synthesis of SSEA-1.<sup>23</sup> To evaluate the effect of FUT9 administration on the expression of SSEA-1 in the lungs of BPD mice, immunohistochemistry of the lungs of FUT9-injected BPD mice was performed using the stem cell surface marker, SSEA-1 (Fig. 5c, d). We demonstrate specific green fluorescent signal of SSEA-1 in the RA lungs, which was significantly decreased in BPD group. However, administration of

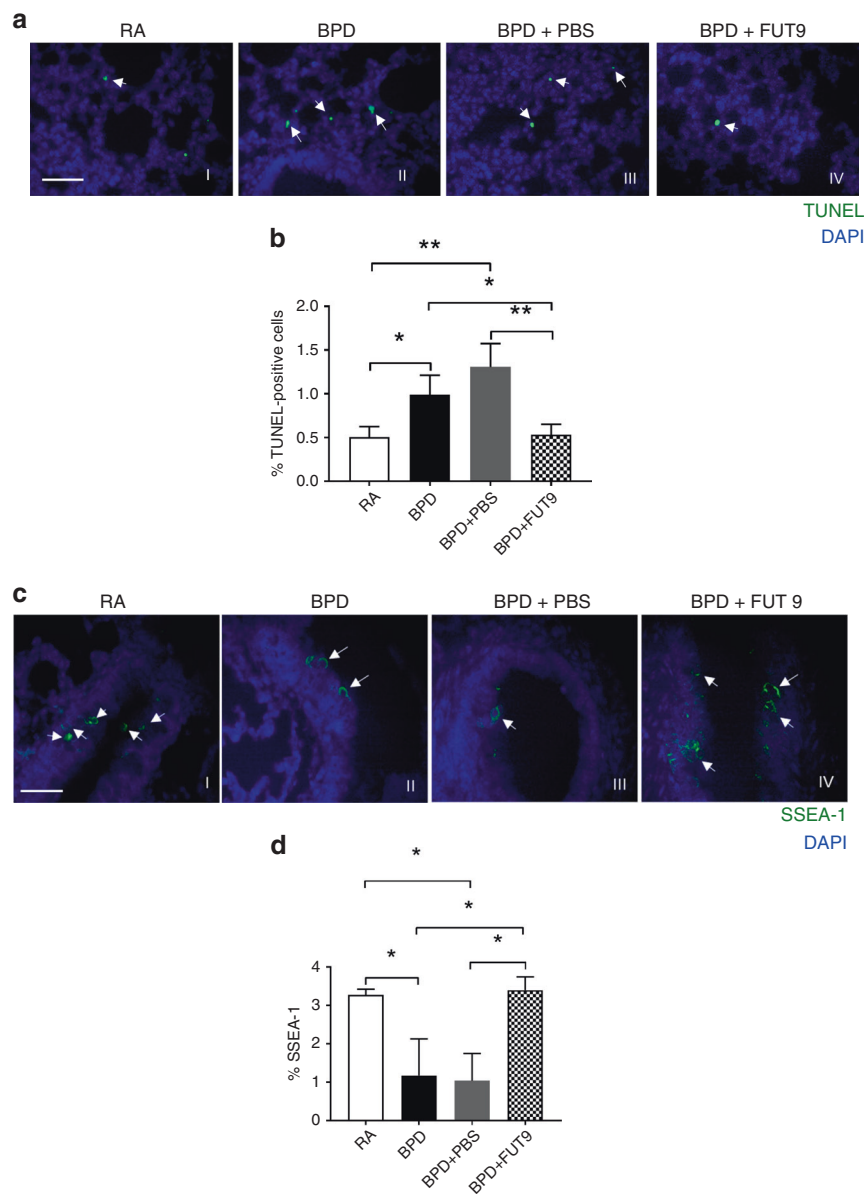


**Fig. 5** FUT9 treatment decreases cell death and increases the expression of SSEA-1 in the lungs of BPD mouse model. **a** Representative TUNEL immunofluorescence images of lung from the four experimental groups, RA (I), BPD (II), BPD + PBS (III), BPD + FUT9 (IV). TUNEL-positive cells are labeled with FITC (green). The nuclei are counterstained with DAPI. Arrows depict TUNEL-positive dead cells in the field. Scale bar: 50  $\mu$ m. **b** Histogram depicting the quantitative analysis of TUNEL-positive cells in the lungs of RA, BPD, and PBS- and FUT9-injected BPD mice. **c** Representative SSEA-1 immunofluorescence images of lung from the four experimental groups, RA (I), BPD (II), BPD + PBS (III), BPD + FUT9 (IV). SSEA-1-positive cells are labeled with FITC (green). The nuclei are counterstained with DAPI. Arrows depict SSEA-1-positive cells in the field. Scale bar: 50  $\mu$ m. **d** Histogram depicting the quantitative analysis of SSEA-1-positive cells in the lungs of RA, BPD, and PBS- and FUT9-injected BPD mice. All values are expressed as mean  $\pm$  SEM;  $N = 3-5$  mice per group; one-way ANOVA with Tukey's post hoc correction; \* $p < 0.05$ ; \*\* $p < 0.01$ .

FUT9 significantly increased the expression of SSEA-1 when compared to that of BPD mice (Fig. 5c, d). No significant increase in SSEA-1 expression was detected in the vehicle/PBS-injected group, thus depicting specific increase in the expression of SSEA-1 in the FUT9-injected BPD mice. SSEA-1 has been shown to be present on human granulocytes, such as neutrophils in a FUT9-dependent manner.<sup>24</sup> Based on the increase in neutrophil infiltration during BPD, we questioned the source of SSEA-1 expression. To rule out the contribution of murine neutrophilic SSEA-1 expression, we assessed SSEA-1 expression on neutrophils in our different experimental conditions. Consistent with the literature, we found no expression of SSEA-1 on mouse neutrophils (Supplementary Fig. S4E online). No changes were

noted in SSEA-1 expression also in macrophages and dendritic cells (data not shown). SSEA-1 expression pattern is different in humans than mice.<sup>25</sup> In mice, SSEA-1 is expressed on stem cells and lost upon differentiation. In stark contrast, humans upregulate SSEA-1 upon differentiation and not during stem cell stages.<sup>26</sup> This suggests that FUT9 regulates the proliferation of stem cells in our murine BPD model via modulation of the expression of SSEA-1.

We further demonstrated effects of FUT9 treatment on lung inflammation by evaluating cytokine expression levels in different experimental groups. Western blotting was performed for inflammation markers interleukin-6 (IL-6) and IL-1 $\beta$  (Supplementary Fig. S5A online). There was increased expression of IL-6 in BPD and BPD + PBS groups, and increased the expression of IL-1 $\beta$  in

BPD, BPD + PBS, and BPD + FUT9 groups in comparison to RA. No significant increase in the expression of IL-6 and IL-1 $\beta$  was observed between RA- and RA + FUT9-injected groups. FUT9 administration in BPD mice did not change inflammatory IL-6 and IL-1 $\beta$  expression levels (Supplementary Fig. S5B, C online). In whole lung tissue, there was an equivalent increase in neutrophil counts in the sham- and FUT9-treated BPD-induced model. Finally, absolute number of alveolar macrophages remained unaltered in all conditions (Supplementary Fig. S5D online).

To determine FUT9 effect on lung angiogenesis, we performed Western blotting of the lung lysates to determine Ang2/Ang1 ratio (Supplementary Fig. S6A–D online). We observed that there was an increase in Ang2/Ang1 ratio in FUT9-injected groups, suggesting increased formation of blood vessels. No significant change in Ang1 levels was observed. FUT9 treatment did not reverse PH and RVH in hyperoxia-induced lung injury (Supplementary Fig. S7 online). Echocardiography was done to determine the ratio between pulmonary artery acceleration time (PAAT) and PA ejection time (PAET). There was no significant increase in PAAT/PAET ratio; hence, no reversal of PH was observed (data not shown).

## DISCUSSION

Stem cells are essential for normal organ development, maintenance, and repair. It is therefore biologically plausible that exhaustion or dysfunction of resident endogenous lung stem cells contributes to the inability of the immature lung to repair itself.<sup>27</sup> The ability to enhance endogenous stem cell capacity to regenerate lung tissue is important for the treatment of BPD.<sup>28,29</sup> We analyzed the effect of hyperoxia on the expression of endogenous PSC marker SSEA-1 and its upstream and downstream proteins, present in the lung, which are involved in the proliferation pathway. We demonstrate that the enzyme of SSEA-1, FUT9, is an important molecule for the therapy of BPD, which increases the expression of SSEA-1. Administration of FUT9 in BPD mouse model demonstrated that FUT9 plays an immunomodulatory role in the progression of BPD by reducing lung damage, increasing proliferation and decreasing lung airway (but not parenchymal) inflammatory responses.

The respiratory tract contains several sources of endogenous adult stem cells that self-renew and generate progeny to regenerate the lung epithelium and contribute to the rapid repair of the alveolar surface after injury.<sup>6,30–32</sup> Neonatal lung SSEA-1+ cells possess self-renewal, clonogenicity, and multipotency ability and differentiate into pneumocytes and tracheal epithelial cells.<sup>8</sup> SSEA-1+ cells are defined as progenitor/stem cells for all differentiated airway epithelial cells. Other groups have shown that the neonatal mice population of putative progenitor cells express CCSP, Sca-1, SSEA-1, and Oct 4, and these differentiate into type I and type II alveolar epithelial cells, which corresponds to our SSEA-1/SP-C colocalization result.<sup>33</sup> Another study show that prolonged Sox2 expression resulted in the reversal of the type II cells towards a more embryonic, precursor-like cell, being positive for the stem cell marker SSEA-1.<sup>34</sup> All these indicate that if SSEA-1 progenitor cells differentiate, they are directed towards type II alveolar epithelial cells. We demonstrate that RA mouse lungs have ~3% of SSEA-1-positive cells, which is comparable to those reported earlier in the pulmonary cell suspensions in the neonatal airways.<sup>8</sup> We also demonstrate that SSEA-1, which is an epithelial progenitor cell marker, colocalizes with SP-C, a specific epithelial cell marker of alveolar type II cells, and on hyperoxia exposure, SSEA-1/SP-C double-positive cells are decreased in BPD lungs compared to RA counterparts, thus depicting decreased stem cell pools in the BPD mice. Decreased expression of SSEA-1 was also observed in an additional VEGF TG (+) PN7 RA model of lung injury.

Another endogenous stem cell marker club cell secretory protein 16 (CC16; previously referred to as Clara cell secretory

protein) expression in bronchiolar epithelium has been associated with hyperoxia-induced epithelial cell damage.<sup>35</sup> Studies show weak expression of CC16 in asthmatic lung tissue compared with healthy lung tissue.<sup>36</sup> However, in SSEA-1+ PSC recipients, CC16 was strongly expressed.<sup>8</sup> Similarly, lung endothelial colony-forming cells isolated from oxygen-exposed neonatal rats showed profound reductions in their clonogenic and angiogenic potential, a distinct sign of functional stem cell impairment.<sup>37</sup> Therefore, we predicted that neonatal SSEA-1+ pulmonary stem cells might be an important marker in physiological and pathological context associated with BPD. We report high levels of SSEA-1 in RA mouse lungs, which decreases significantly in BPD mouse, suggesting that BPD is associated with decreased levels of SSEA-1. We demonstrate decrease in SSEA-1 expression in human BPD and RDS lung samples compared to their term control counterparts, suggesting lung SSEA-1+ cells to be a potentially useful airway inflammatory biomarker in the diagnosis and management of BPD.

The alveolar growth impairment in BPD is due to disruption of secondary septa formation as well as a matrix that has not been fully formed. At a cellular level, these abnormalities are presumed to be due to defective elastogenesis and extracellular matrix (ECM) remodeling,<sup>38</sup> altered alveolar epithelial–mesenchymal interactions, and impaired development of lung microvasculature.<sup>39,40</sup> These changes may affect the endogenous PSC populations, making it difficult to repair the immature lung and thus contributing to the development of BPD. SSEA-1 has been shown to bind to hyaluronan that is essential for stabilizing and remodeling the ECM, which is an integral part of the developing lung, during inflammatory disease processes such as arthritis.<sup>13,41</sup> We demonstrate that SSEA-1 expression is decreased in BPD and RDS human lungs and in BPD mouse, indicating that decrease in SSEA-1 might alter the epithelial cell–ECM interactions decreasing epithelial cell migration and proliferation and differentiation of repairing cells, leading to decreased restoration of the lung injury.

Mice have three functional *Fut* genes, *Fut4*, *Fut7*, and *Fut9*, corresponding to the human *FUT4*, *FUT7*, and *FUT9* genes. Out of these three genes, only *Fut9* has an amino acid sequence that is highly conserved in the human counterpart *FUT9*.<sup>42</sup> Utilizing the high homology between the mouse and human *FUT9*, we administered rhFUT9 to an experimental mouse model of hyperoxia-induced injury that replicates human BPD.<sup>13,14,41</sup>

BALF analysis showed decreased inflammatory cells in the FUT9-treated BPD mice, accompanied by no significant change in the inflammatory cytokine levels in the lung tissue, compared to BPD mice. The mechanism for this differential response is beyond the scope of this manuscript. Interestingly, we also found that in FUT9-treated BPD mice there was decreased cell death, but no change in inflammatory cells in lung parenchymal tissue, compared to BPD mice. Similar juxtaposed observation of hyperoxia-induced inflammation and lung injury was also seen in our previous study with IL-13-null mutants,<sup>43</sup> where null mutations of IL-13, while diminishing hyperoxia-induced inflammation, increased hyperoxia-induced DNA injury and cell death, demonstrating that hyperoxia-induced injury or death cannot be attributed solely to local tissue inflammation or vice versa.

We evaluated the efficacy of FUT9 in the treatment of BPD at a developmentally appropriate window. The saccular stage of murine lung development occurs between embryonic day 18 and PN4. Therefore, the term mouse represents a developmental stage resembling that of a human preterm neonate between 24 and 28 weeks. Our results are in the context of the experimental model of severe BPD,<sup>13,14</sup> oxygen exposure in the saccular stage, from birth till PN4, as compared to the models of hyperoxia-induced acute lung injury, where exposure to 60–100% oxygen is up to 2–4 weeks in mouse, throughout saccular and alveolar stages,<sup>44</sup> which corresponds to the developmental stages extending from preterm to adolescence in humans. These are



important factors when assessing translational significance as modeling needs to be developmentally appropriate to mimic human BPD as closely as possible. Additionally, although term mouse lungs, in the saccular stage, are competent for proper gas exchange, human preterm neonates often require supplemental oxygen and surfactant administration. The model used in this study could represent a human preterm neonate who has been adequately administered prenatal steroids (which results in lung maturation) and are exposed to high concentration of supplemental oxygen.<sup>41</sup> Our model represents the pathological pulmonary characteristics of the lungs of human neonates with BPD.

SSEA-1-containing glycans can modulate the expression of several glycoconjugates involved in notch signaling to upregulate proliferation and self-renewal.<sup>19</sup> FUT9 is a key enzyme for the synthesis of the SSEA-1 carbohydrate epitope. FUT9 knockdown in mouse NSC impaired Msi-1 expression and NSC proliferation.<sup>19</sup> We demonstrate that hyperoxia markedly decreased expression of SSEA-1 in the lungs of BPD mice. This correlates with earlier studies showing markedly decreased expression of stem cell markers, like Notch-1 on hyperoxia exposure or other lung injury diseases.<sup>45,46</sup> On administration of FUT9, SSEA-1 increases and up-regulates endogenous stem cell proliferation probably by modulating the expression of glycoconjugates involved in Notch signaling. We demonstrate that i.p. administration of rhFUT9 significantly attenuates neonatal hyperoxia-induced BPD lung pathology, in part, via decreased cell death and increased proliferation of pulmonary cells. The present study indicates that FUT9 promotes stem cell proliferation by modulation of SSEA-1. SSEA-1 expression is upregulated on administration of FUT9, which accounts for the proliferative effect of pulmonary cells. Future studies on understanding the molecular mechanisms of different components of SSEA-1 pathway will shed light on exploring the novel therapeutic approaches for hyperoxia-induced lung injury.

Nevertheless, there are limitations of this study that need to be addressed before translation of the therapy to the clinical setting. Only one dose of rhFUT9 was selected for these studies based on earlier studies and there is no dose–response data. More preclinical studies on larger animals are needed to standardize and identify a range of doses and timing for the intervention along with the functional assays. More mechanistic information is needed to better understand how FUT9 works as a preventive or early therapeutic approach for BPD. This will enable us to determine the best clinical candidates with BPD for FUT9 therapy.

In conclusion, we demonstrate that administration of rhFUT9, an enzyme of endogenous stem cell marker SSEA-1, improves BPD pathology of lungs, reduces lung airway inflammation, alveolar–capillary leak, and cell death in the BPD mouse model. We provide a quantitative assessment of therapeutic effects of FUT9 in vivo in terms of lung morphometry in BPD. Our findings suggest FUT9 as an attractive and plausible means to regulate SSEA-1 pathway and produce a robust therapeutic effect in vivo. Improved knowledge about the characterization, localization, and mechanism of action of endogenous lung progenitor cells in lung development and repair after injury could lead to the development of novel endogenous stem cell therapy strategies in lung disease.

#### ACKNOWLEDGEMENTS

We thank Gloria Pryhuber, M.D., at the University of Rochester, New York, for kindly providing human lung sections. This study was funded by grants to V.B. from Drexel University (fund #: 270926 and 282656).

#### AUTHOR CONTRIBUTIONS

S.C. and V.B. conceived and designed the study; S.C., Y.M.N., D.S., O.K.K., V.P., A.J.C., and S.A. contributed in the collection and assembly of data; S.C., O.K.K., A.J.C., and V.B. performed data analysis and interpretation; S.C. drafted the initial manuscript; S.C.,

Y.M.N., D.S., O.K.K., V.P., A.J.C., S.A., and V.B. were involved in the editing and revision of manuscript. All authors approved the final version of the submitted manuscript.

#### ADDITIONAL INFORMATION

The online version of this article (<https://doi.org/10.1038/s41390-020-0891-9>) contains supplementary material, which is available to authorized users.

**Competing interests:** The authors declare no competing interests.

**Patient consent:** Informed consent was obtained, and the collection and processing of the human lung samples was approved by the National Supervisory Authority for Welfare and Health in Finland (S.A.) and the University of Rochester Institutional Review Board (Gloria Pryhuber, MD).

**Publisher's note** Springer Nature remains neutral with regard to jurisdictional claims in published maps and institutional affiliations.

#### REFERENCES

- Davidson, L. M. & Berkelhamer, S. K. Bronchopulmonary dysplasia: chronic lung disease of infancy and long-term pulmonary outcomes. *J. Clin. Med.* **6**, 4 (2017).
- Bhandari, V. *Bronchopulmonary Dysplasia (Respiratory Medicine)* 1st edn (Humana Press, a brand of Springer, New York; ATS, American Thoracic Society, 2016).
- Jobe, A. H. Mechanisms of lung injury and bronchopulmonary dysplasia. *Am. J. Perinatol.* **33**, 1076–1078 (2016).
- Alphonse, R. S., Rajabali, S. & Thebaud, B. Lung injury in preterm neonates: the role and therapeutic potential of stem cells. *Antioxid. Redox Signal.* **17**, 1013–1040 (2012).
- Hogan, B. L. et al. Repair and regeneration of the respiratory system: complexity, plasticity, and mechanisms of lung stem cell function. *Cell Stem Cell* **15**, 123–138 (2014).
- Kotton, D. N. & Morrisey, E. E. Lung regeneration: mechanisms, applications and emerging stem cell populations. *Nat. Med.* **20**, 822–832 (2014).
- Rock, J. R. & Hogan, B. L. Epithelial progenitor cells in lung development, maintenance, repair, and disease. *Annu. Rev. Cell Dev. Biol.* **27**, 493–512 (2011).
- Chiu, C. J., Ling, T. Y. & Chiang, B. L. Lung-derived SSEA-1(+) stem/progenitor cells inhibit allergic airway inflammation in mice. *Allergy* **70**, 374–383 (2015).
- Chaubey, S. & Wolfe, J. H. Transplantation of CD15-enriched murine neural stem cells increases total engraftment and shifts differentiation toward the oligodendrocyte lineage. *Stem Cells Transl. Med.* **2**, 444–454 (2013).
- Yanagisawa, M. & Yu, R. K. The expression and functions of glycoconjugates in neural stem cells. *Glycobiology* **17**, 57R–74R (2007).
- Solter, D. & Knowles, B. B. Monoclonal antibody defining a stage-specific mouse embryonic antigen (SSEA-1). *Proc. Natl Acad. Sci. USA* **75**, 5565–5569 (1978).
- Kudo, T. et al. Expression cloning and characterization of a novel murine  $\alpha$ 1,3-fucosyltransferase, mFuc-TIX, that synthesizes the Lewis x (CD15) epitope in brain and kidney. *J. Biol. Chem.* **273**, 26729–26738 (1998).
- Sun, H. et al. Small molecular modulation of macrophage migration inhibitory factor in the hyperoxia-induced mouse model of bronchopulmonary dysplasia. *Respir. Res.* **14**, 27 (2013).
- Chaubey, S. et al. Early gestational mesenchymal stem cell secretome attenuates experimental bronchopulmonary dysplasia in part via exosome-associated factor TSG-6. *Stem Cell Res Ther.* **9**, 173–198 (2018).
- Syed, M. A., Choo-Wing, R., Homer, R. J. & Bhandari, V. Role of nitric oxide isoforms in vascular and alveolar development and lung injury in vascular endothelial growth factor overexpressing neonatal mice lungs. *PLOS ONE* **11**, e0147588 (2016).
- Willis, G. R. et al. Mesenchymal stromal cell exosomes ameliorate experimental bronchopulmonary dysplasia and restore lung function through macrophage immunomodulation. *Am. J. Respir. Crit. Care Med.* **197**, 104–116 (2018).
- Snyder, J. M. et al. Alveolarization in retinoic acid receptor-beta-deficient mice. *Pediatr. Res.* **57**, 384–391 (2005).
- Yagi, H., Yanagisawa, M., Kato, K. & Yu, R. K. Lysosome-associated membrane protein 1 is a major SSEA-1-carrier protein in mouse neural stem cells. *Glycobiology* **20**, 976–981 (2010).
- Yagi, H., Saito, T., Yanagisawa, M., Yu, R. K. & Kato, K. Lewis X-carrying N-glycans regulate the proliferation of mouse embryonic neural stem cells via the Notch signaling pathway. *J. Biol. Chem.* **287**, 24356–24364 (2012).
- Imai, T. et al. The neural RNA-binding protein Musashi1 translationally regulates mammalian numb gene expression by interacting with its mRNA. *Mol. Cell. Biol.* **21**, 3888–3900 (2001).
- Okano, H. et al. Function of RNA-binding protein Musashi-1 in stem cells. *Exp. Cell Res.* **306**, 349–356 (2005).

22. Shimoda, Y. et al. Pax6 controls the expression of Lewis x epitope in the embryonic forebrain by regulating alpha 1,3-fucosyltransferase IX expression. *J. Biol. Chem.* **277**, 2033–2039 (2002).
23. Nishihara, S. et al.  $\alpha$ 1,3-Fucosyltransferase IX (Fut9) determines Lewis X expression in brain. *Glycobiology* **13**, 445–455 (2003).
24. Nakayama, F. et al. CD15 expression in mature granulocytes is determined by  $\alpha$ 1,3-fucosyltransferase IX, but in promyelocytes and monocytes by  $\alpha$ 1,3-fucosyltransferase IV. *J. Biol. Chem.* **276**, 16100–16106 (2001).
25. Fox, N., Damjanov, I., Knowles, B. B. & Solter, D. Immunohistochemical localization of the mouse stage-specific embryonic antigen 1 in human tissues and tumors. *Cancer Res.* **43**, 669–678 (1983).
26. Draper, J. S., Pigott, C., Thomson, J. A. & Andrews, P. W. Surface antigens of human embryonic stem cells: changes upon differentiation in culture. *J. Anat.* **200**, 249–258 (2002).
27. Mercado, N., Ito, K. & Barnes, P. J. Accelerated ageing of the lung in COPD: new concepts. *Thorax* **70**, 482–489 (2015).
28. O'Reilly, M. & Thebaud, B. The promise of stem cells in bronchopulmonary dysplasia. *Semin. Perinatol.* **37**, 79–84 (2013).
29. Mobius, M. A. & Thebaud, B. Bronchopulmonary dysplasia: where have all the stem cells gone?: origin and (potential) function of resident lung stem cells. *Chest* **152**, 1043–1052 (2017).
30. Lee, J., Reddy, R., Barsky, L., Weinberg, K. & Driscoll, B. Contribution of proliferation and DNA damage repair to alveolar epithelial type 2 cell recovery from hyperoxia. *Am. J. Physiol. Lung Cell. Mol. Physiol.* **290**, L685–L694 (2006).
31. Kim, C. F. et al. Identification of bronchioalveolar stem cells in normal lung and lung cancer. *Cell* **121**, 823–835 (2005).
32. Rawlins, E. L. Lung epithelial progenitor cells: lessons from development. *Proc. Am. Thorac. Soc.* **5**, 675–681 (2008).
33. Ling, T. Y. et al. Identification of pulmonary Oct-4<sup>+</sup> stem/progenitor cells and demonstration of their susceptibility to SARS coronavirus (SARS-CoV) infection in vitro. *Proc. Natl Acad. Sci. USA* **103**, 9530–9535 (2006).
34. Kapere, O. J. et al. Differentiated type II pneumocytes can be reprogrammed by ectopic Sox2 expression. *PLoS ONE* **9**, 9–12 (2014).
35. Johnston, C. J., Mango, G. W., Finkelstein, J. N. & Stripp, B. R. Altered pulmonary response to hyperoxia in Clara cell secretory protein deficient mice. *Am. J. Respir. Cell. Mol. Biol.* **17**, 147–155 (1997).
36. Shijubo, N. et al. Serum levels of Clara cell 10-kDa protein are decreased in patients with asthma. *Lung* **177**, 45–52 (1999).
37. Alphonse, R. S. et al. Existence, functional impairment, and lung repair potential of endothelial colony-forming cells in oxygen-induced arrested alveolar growth. *Circulation* **129**, 2144–2157 (2014).
38. Bourbon, J., Boucherat, O., Chailley-Heu, B. & Delacourt, C. Control mechanisms of lung alveolar development and their disorders in bronchopulmonary dysplasia. *Pediatr. Res.* **57**, 38R–46R (2005).
39. Bhatt, A. J. et al. Disrupted pulmonary vasculature and decreased vascular endothelial growth factor, Flt-1, and TIE-2 in human infants dying with bronchopulmonary dysplasia. *Am. J. Respir. Crit. Care Med.* **164**, 1971–1980 (2001).
40. Collins, J. J. & Thebaud, B. Lung mesenchymal stromal cells in development and disease: to serve and protect? *Antioxid. Redox Signal.* **21**, 1849–1862 (2014).
41. Berger, J. & Bhandari, V. Animal models of bronchopulmonary dysplasia. The term mouse models. *Am. J. Physiol. Lung Cell. Mol. Physiol.* **307**, L936–L947 (2014).
42. Kaneko, M. et al. Alpha1,3-fucosyltransferase IX (Fuc-TIX) is very highly conserved between human and mouse; molecular cloning, characterization and tissue distribution of human Fuc-TIX. *FEBS Lett.* **452**, 237–242 (1999).
43. Bhandari, V., Choo-Wing, R., Homer, R. J. & Elias, J. A. Increased hyperoxia-induced mortality and acute lung injury in IL-13 null mice. *J. Immunol.* **178**, 4993–5000 (2007).
44. Lee, C. et al. Exosomes mediate the cytoprotective action of mesenchymal stromal cells on hypoxia-induced pulmonary hypertension. *Circulation* **126**, 2601–2611 (2012).
45. Tilley, A. E. et al. Down-regulation of the notch pathway in human airway epithelium in association with smoking and chronic obstructive pulmonary disease. *Am. J. Respir. Crit. Care Med.* **179**, 457–466 (2009).
46. Zhang, Q., Chang, L., Liu, H., Rong, Z. & Chen, H. Relationship between Notch receptors and hyperoxia-induced lung injury in newborn rats. *J. Huazhong Univ. Sci. Technol. Med. Sci.* **25**, 155–158 (2005).